https://doi.org/10.5194/tc-2019-97
Preprint. Discussion started: 4 June 2019

The Cryosphere Discussions

Validating modeled critical crack length for crack propagation in the snow cover model SNOWPACK

Bettina Richter[1], Jürg Schweizer[1], Mathias W. Rotach[2], and Alec van Herwijnen[1]

[1]WSL Institute for Snow and Avalanche Research SLF, Davos, Switzerland
[2]Institute for Atmospheric and Cryospheric Sciences, University of Innsbruck, Innsbruck, Austria

Correspondence: Bettina Richter (bettina.richter@slf.ch)

Abstract. Data on snow stratigraphy and snow instability are of key importance for avalanche forecasting. Snow cover models can improve the spatial and temporal resolution of such data, especially if they also provide information on snow instability. Recently, a new stability criterion, namely a parameterization for the critical crack length, was implemented into the snow cover model SNOWPACK. To validate and improve this parameterization, we therefore used data from three years of field experiments performed close to two automatic weather station above Davos, Switzerland. Monitoring the snowpack on a weekly basis allowed to investigate limitations of the model. Based on 145 experiments we replaced two variables of the original parameterization, which were not sufficiently well modeled, with a fit factor thereby decreasing the normalized root mean square error from 1.80 to 0.28. With this fit factor, the improved parameterization accounts for the grain size resulting in lower critical crack lengths for snow layers with larger grains. This also improved an automatic weak layer detection method using a simple local minimum by increasing the probability of detection from 0.26 to 0.91 and decreased the false alarm ratio from 0.89 to 0.47.

1 Introduction

Snow slab avalanches are hazardous and can threaten people and infrastructure. Each year, around a 100 avalanche fatalities occur in the European Alps (Techel et al., 2016). Whether avalanche release is likely, largely depends on snow layering, in particular the complex interaction between slab layers and a so-called weak layer (Schweizer et al., 2008). Such weak layers often form near or at the snow surface and, if subsequently covered by a snowfall, can sometimes persist throughout the season.

Dry-snow slab avalanches start with a failure in the weak layer resulting in a macroscopic crack. If this crack reaches a critical size, the crack will rapidly propagate outward (e.g. McClung and Schweizer, 1999; Schweizer et al., 2003a). Hence, two key processes in avalanche release are failure initiation and crack propagation (Reuter et al., 2015; Schweizer et al., 2016a). Recently, a third criterion based on the tensile strength of the slab was suggested, which in large parts determines whether the slab can support crack propagation (Reuter and Schweizer, 2018). The type and location of weak layers found in a snowpack and whether a crack is prone to propagate are thus some of the crucial questions when assessing snow instability. Therefore, snow cover stratigraphy is considered an important contributing factor in avalanche forecasting (Schweizer et al., 2003a).

https://doi.org/10.5194/tc-2019-97
Preprint. Discussion started: 4 June 2019

Snow stratigraphy information is traditionally obtained with manually observed snow profiles, where each layer is characterized by grain type, grain size and hand hardness (Fierz et al., 2009). Manually observed snow profiles are often completed with snow instability tests (e.g. Schweizer and Jamieson, 2010). However, data on snow stratigraphy and snow instability are rare point observations which are very time consuming and sometimes dangerous to obtain. Spatial and temporal improvement of such data can only be made through numerical snow cover modeling (e.g. Lafaysse et al., 2013).

Crocus (Brun et al., 1992; Vionnet et al., 2012) and SNOWPACK (Lehning et al., 2002; Wever et al., 2015) are detailed snow cover models which also provide snow instability information (Schweizer et al., 2006; Lehning et al., 2004; Vernay et al., 2015). The French model chain SAFRAN-Crocus-MEPRA (SCM) predicts the regional avalanche danger (Durand et al., 1999). Crocus is driven with input of the meteorological model SAFRAN and the stratigraphy on virtual slopes for a range of elevations and aspects are simulated. The expert system MEPRA combines various stability indices with a set of rules to evaluate the simulated snow stratigraphy in terms of stability classes and derives the avalanche danger (Giraud and Navarre, 1995). However, the avalanche danger is generally very difficult to validate (Schweizer et al., 2003b).

The snow cover model SNOWPACK is driven with data from automatic weather stations. Stability indices are then calculated from modeled snow stratigraphy, i.e. modeled layer properties. Several stability indices have been implemented in SNOWPACK, in particular the natural stability index SN38 and the skier-stability index SK38 (Lehning et al., 2004; Monti et al., 2016). Both stability indices relate to failure initiation and are based on the ratio of the shear strength of a weak layer to the load of the overlaying slab and, for SK38, the approximate stress due to a skier (Föhn, 1987; Jamieson and Johnston, 1998). Weak layer shear strength is parameterized using emperical relationships from shear frame measurements relating snow density and grain type (e.g. Chalmers, 2001; Jamieson and Johnston, 2001) and calculated in SNOWPACK for each modeled snow layer (Lehning et al., 2004). Recently, a parameterization for the critical crack length, which relates to the onset of crack propagation, was suggested by Gaume et al. (2017) and implemented into SNOWPACK. A preliminary comparison of measured and modeled critical crack lengths for one particular field day suggested a good agreement. Schweizer et al. (2016b) monitored the temporal evolution of a weak layer during the winter season 2014-2015 above Davos, Switzerland. They compared the temporal evolution of the critical crack length observed with field experiments to the critical crack length predicted by SNOWPACK. Although SNOWPACK reproduced the overall trend fairly well, the seasonal increase was too pronounced. They attributed these discrepancies to an overestimation of weak layer density in SNOWPACK, however their analysis only included one type of weak layer.

In this study, we will investigate the performance and limitations of the SNOWPACK model to predict the critical crack length. We will use a dataset containing weekly field measurements. During three winter seasons, 2014-2017, we tracked persistent weak layers with time at different locations and conducted measurements of critical crack lengths. This dataset was used to validate and improve the parameterization of the critical crack length suggested by Gaume et al. (2017). The new formulation additionally considers the micro-structural parameter grain size from the snow cover model. It allows for a better representation of the temporal evolution of the critical crack length and automatic weak layer detection.

https://doi.org/10.5194/tc-2019-97
Preprint. Discussion started: 4 June 2019

2 Methods

2.1 Field sites

We collected data during three winter seasons, from 2014-2015 to 2016-2017, at two flat field sites above Davos, Switzerland. Both sites are relatively sheltered from wind and equipped with an automatic weather station (AWS) measuring snow depth, air temperature, relative humidity, wind speed, wind direction, incoming and outgoing short- and longwave radiation. The Weissfluhjoch (WFJ; 46.830° N, 9.809° E) site is located at 2536 m a.s.l. and the Wannengrat (WAN7; 46.808° N, 9.788° E) site is located at 2442 m a.s.l. about 3 km to the southwest from WFJ; they typically have a similar snowpack.

2.2 Snow profiles and stability tests

At both sites, manual snow profiles were recorded on an almost weekly basis between January and March (Table 1). Data on hand hardness, temperature, density, grain type and grain size were recorded according to Fierz et al. (2009). Density was measured either for each individual snow layer or every 3 cm in a vertical profile.

Manual snow profiles were complemented with stability tests, namely the Compression Test (CT; van Herwijnen and Jamieson, 2007), the Extended Compression Test (ECT; Simenhois and Birkeland, 2009) and the Propagation Saw Test (PST; Gauthier and Jamieson, 2008a). In a CT, an isolated column of snow of 30 cm $\times$ 30 cm is progressively loaded by tapping up to 30 times on a shovel; 10 times from the wrist, 10 times from the elbow and 10 times from the shoulder (van Herwijnen and Jamieson, 2007). If a failure occurs, the number of taps is recorded as well as a qualitative description of the fracture type, as suggested in van Herwijnen and Jamieson (2007). An ECT is very similar to a CT. The main difference is that the column is 30 cm $\times$ 90 cm and when a failure occurs the number of taps and the propagation distance are recorded, as described in Simenhois and Birkeland (2009). Both these tests are widely used to identify weak layers and qualify the failure. A PST, on the other hand, is a fracture mechanical field test used to assess the critical crack length required for rapid crack propagation in an a priori known weak layer (van Herwijnen and Jamieson, 2005; Sigrist and Schweizer, 2007; Gauthier and Jamieson, 2006). It consists of an isolated column of 30 cm width and a variable length of at least 120 cm. A failure in the weak layer is initiated by cutting the weak layer with a snow saw until the crack propagates. The length at which the crack propagated is called the critical crack length r_c. The critical crack length as well as the propagation distance are recorded. On each of the 47 measurement days (Table 1), we performed CTs, ECTs, and one to five PSTs per weak layer. In total, 145 PST experiments were conducted, yielding a data set of 68 mean critical crack lengths for 7 different weak layers. Weak layers were coded after their grain type (GT) according to Fierz et al. (2009) and burial date (YYMMDD) with a code GTYYMMDD. For the comparison with SNOWPACK simulations, the mean r_c value of all PSTs was taken, measured for any given weak layer on a particular day.

https://doi.org/10.5194/tc-2019-97
Preprint. Discussion started: 4 June 2019

Table 1. Overview of field data and Propagation Saw Tests (PST) available for validation. See Sect. 2.1 for the sites WAN7 and WFJ.

Year	Field site	Number of persistent weak layers	Number of field days (Jan-Apr)	Number of PST experiments
2014-2015	WAN7	2	8	43
2015-2016	WAN7	1	7	27
2015-2016	WFJ	2	8	22
2016-2017	WAN7	1	10	33
2016-2017	WFJ	1	14	20

2.3 SNOWPACK

We used the snow cover model SNOWPACK (version 3.4.1, revision 1473) to simulate the snow stratigraphy (Bartelt and Lehning, 2002). The model was driven with AWS data at both sites, using air temperature, relative humidity, snow surface temperature, wind speed, short- and longwave radiation. For the WAN7 site the snow cover mass balance was enforced with the increment of measured snow depth. For the WFJ site additional data from a heated rain gauge was used to estimate the occurrence of rain (WSL Institute for Snow and Avalanche Research SLF, 2015). At both sites, Neumann boundary conditions were used at the snow surface and a constant geothermal heat flux of 0.06 W m^{-2} at the bottom of the snowpack was assumed. The simulation time step was 15 min and the output was written for every day.

Based on these meteorological input data, SNOWPACK simulates the formation and metamorphism of snow layers. Each layer therefore has different properties, mainly characterized by its density, temperature, grain type and grain size. Simulated snow layers were tagged with their deposition date and added to the output. Using the deposition date in SNOWPACK and the burial date of observed weak layers in the manual snow profiles allowed for an unambiguous comparison without requiring any layer matching. A given weak layer in the manual profile corresponds to the uppermost layer in the simulation with a deposition date older than the burial date of the observed weak layer. For buried surface hoar, the lowermost layer with the same burial date was taken in the simulations.

From simulated layer properties, snow mechanical properties required for the parameterization of the critical crack length (see Section 2.4) are computed in SNOWPACK. The elastic modulus of the slab, E, was derived from mean slab density ρ_{sl} following Scapozza (2004):

$$E = 5.07 \times 10^9 \left(\frac{\rho_{sl}}{\rho_{ice}} \right)^{5.13} \text{Pa}, \tag{1}$$

with $\rho_{ice} = 917\,\text{kg m}^{-3}$ the density of ice. For the shear strength τ_p, different parameterizations for each grain type are implemented (Figure 1). For all grain types except for SH (see caption of Fig. 1 for the acronyms of different grain types), τ_p solely depends on ρ_{wl} through a power law function $\tau_p = a \left(\frac{\rho_{wl}}{\rho_{ice}} \right)^b$. For SH, the parametrization of Lehning et al. (2004) was applied, which is a function of age of the weak layer, the normal stress σ_n, slab thickness D_{sl}, snow depth (HS), weak layer thickness D_{wl} and weak layer temperature T_{wl}. The normal stress $\sigma_n = \rho_{sl} g D_{sl}$ is exerted on the weak layer due to the overlying slab,

https://doi.org/10.5194/tc-2019-97
Preprint. Discussion started: 4 June 2019

The Cryosphere Discussions
Open Access
EGU

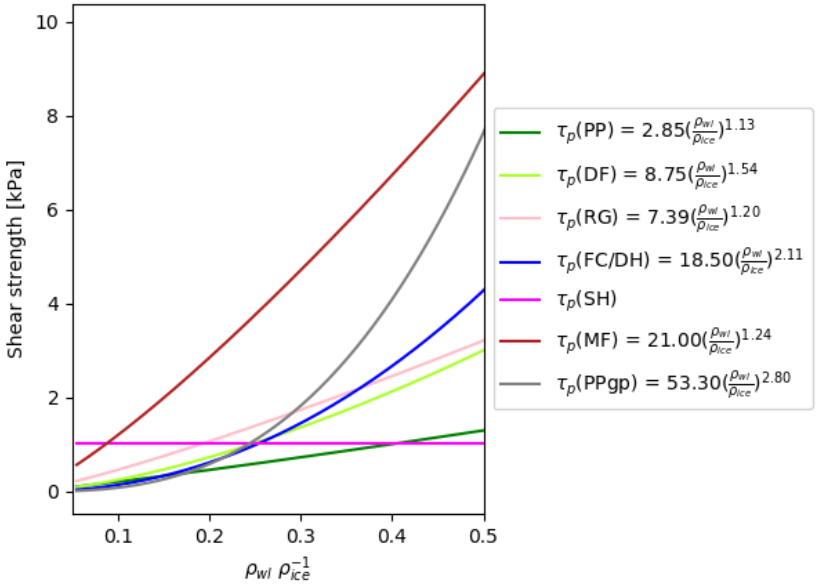

Figure 1. Shear strength as a function of normalized density $\frac{\rho_{wl}}{\rho_{ice}}$ for different grain types as implemented in SNOWPACK. Grain types are precipitation particles (PP), decomposed and fragmented precipitation particles (DF), rounded grains (RG), faceted crystals (FC) and depth hoar (DH), surface hoar (SH), melt forms (MF) and graupel (PPgp).

with the slab thickness D_{sl} and the gravitational acceleration g. In Fig. 1 τ_p is shown for a layer of SH with an age of 7 days, $D_{wl} = 0.01\,\mathrm{m}$, $D_{sl} = 0.5\,\mathrm{m}$, $HS = 1\,\mathrm{m}$, $T_{wl} = -5°\mathrm{C}$, $\rho_{sl} = 200\,\mathrm{kg\,m^{-3}}$ and $\sigma_n = 0.981\,\mathrm{kPa}$.

2.4 Critical crack length parameterization

To estimate the critical crack length from snow mechanical properties, we used the parameterization suggested by Gaume et al. (2017). For a flat field site (slope angle $\theta = 0$) it reduces to:

$$r_c = \Lambda\sqrt{\frac{2\tau_p}{\sigma_n}}, \tag{2}$$

where the characteristic length scale $\Lambda = \sqrt{\frac{E' D_{sl} D_{wl}}{G_{wl}}}$ includes the plain strain elastic modulus of the slab $E' = \frac{E}{(1-\nu^2)}$, the Poisson's ratio of the slab $\nu = 0.2$, and the shear modulus of the weak layer $G_{wl} = 0.2$ MPa, as suggested by Gaume et al. (2017).

All layer properties required in Eq. (2) are available in SNOWPACK. Furthermore, Eq. (2) was also applied to profile data as most properties - i.e. D_{sl}, D_{wl}, ρ_{sl} and ρ_{wl} - were measured directly in the field. Weak layer shear strength and the elastic

https://doi.org/10.5194/tc-2019-97
Preprint. Discussion started: 4 June 2019

modulus of the slab, which were not measured, were derived from measured densities using the same parameterizations as those implemented in SNOWPACK (Eq. (1) and Fig. 1).

2.5 Model performance measures and weak layer detection

We used different performance measures to validate the parameterization for the critical crack length, as well as layer properties from SNOWPACK, namely density and layer thickness. To measure the linear relationship between a modeled value y and a measured value x, we calculated the Pearson correlation coefficient r_p. We considered a level of $p < 0.05$ as significant. To quantify errors, we calculated the normalized root mean square error $NRMSE$:

$$NRMSE = \frac{1}{\bar{x}} \sqrt{\frac{\sum_{i=1}^{n} (x_i - y_i)^2}{n}} \tag{3}$$

where n is the number of measurements (e.g. $n = 68$ is the number of mean values for r_c observed with 145 PST experiments per weak layer and day; see Sect. 2.2) and $\bar{x}$ is the mean of the measurements.

To assess whether the parameterization for the critical crack length implemented in SNOWPACK can be used to automatically identify critical weak layers, we used a local minimum approach to investigate whether the weak layers tested in the field were among the most critical weak layers in SNOWPACK. This approach consisted of ranking layers in SNOWPACK according to their r_c values in ascending order. The most critical layer in SNOWPACK was defined as the layer with the absolute minimum r_c value in the profile. The second critical weak layer had the next lowest local minimum, excluding a range of $5\,\mathrm{cm}$ each above and below the previous weak layer, and so on. Then, the five most critical weak layers in SNOWPACK were compared to those weak layers which were tracked in PST experiments. If a critical weak layer in SNOWPACK was in the range of $\pm 5\,\mathrm{cm}$ of an observed weak layer, it was counted as a detection (d), otherwise as false alarm (fa). Detections and false alarms were counted until either all observed weak layers were found or all five simulated weak layers were compared. If observed weak layers were not detected within the five weakest simulated layers, they were considered not detected (nd). For each field day j, we summed up d, fa and nd. This procedure allowed us to calculate a probability of detection (POD) and a false alarm ratio (FAR) according to Wilks (2011):

$$POD = \frac{\sum_{j=0}^{m} d}{\sum_{j=0}^{m} d + \sum_{j=0}^{m} nd} \tag{4}$$

$$FAR = \frac{\sum_{j=0}^{m} fa}{\sum_{j=0}^{m} d + \sum_{j=0}^{m} fa} \tag{5}$$

where $m = 47$ is the number of field days. Note that $d + nd = n$.

https://doi.org/10.5194/tc-2019-97
Preprint. Discussion started: 4 June 2019

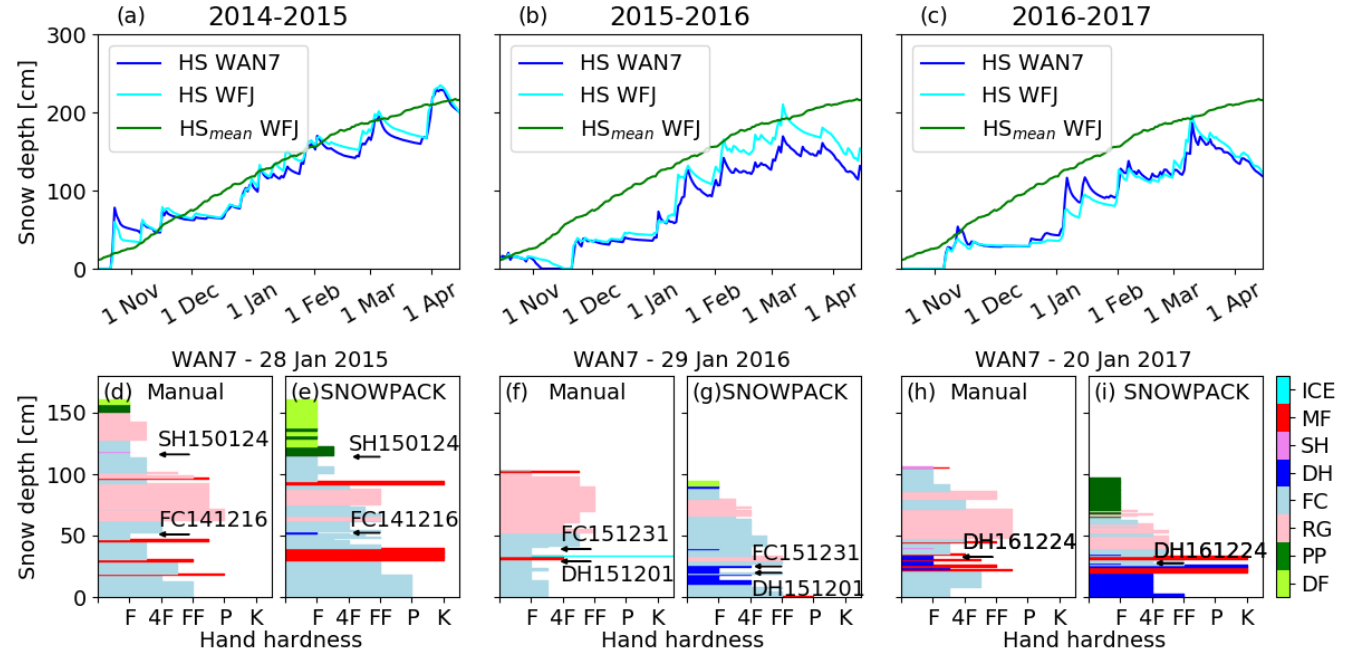

Figure 2. Top: Evolution of snow depth at both field sites for the winter seasons (a) 2014-2015, (b) 2015-2016 and (c) 2016-2017. HS$_{mean}$ is the snow depth at WFJ averaged over 85 years. Bottom: (d,f,h) manually observed snow profile at WAN7 showing hand hardness and grain type (colors) for the end of January each year and (e,g,i) corresponding simulated snow stratigraphy from SNOWPACK. Arrows with labels indicate critical weak layers which were observed in PST experiments. Labels of weak layers were coded after grain type GT and burial date (GTYYMMDD; see caption of Fig. 1 for the acronyms of different grain types)

3 Results

3.1 Winter seasons - weather and snowpack

The snow depth was average during 2014-2015 and generally below average for winter seasons 2015-2016 and 2016-17 (Figure 2). Each winter, one to two pronounced weak layers developed and consistently failed in CT and ECT tests (Figure 3). These persistent weak layers were tracked in PST experiments throughout the season (Table 1). In the following we will give a detailed description of the formation of these weak layers.

Winter 2014-2015

The winter started at the end of October with approximately 60 cm of snow. During the calm weather period starting in mid-November, the snow surface transformed into a layer of faceted crystals, forming a persistent weak layer that was buried by snow in mid-December (FC141216). A layer of surface hoar, which had formed in the region in mid-January, was buried on 24 January 2015 (SH150124) and was subsequently observed in the traditional snow profile on 28 January 2015 (Figure

https://doi.org/10.5194/tc-2019-97
Preprint. Discussion started: 4 June 2019

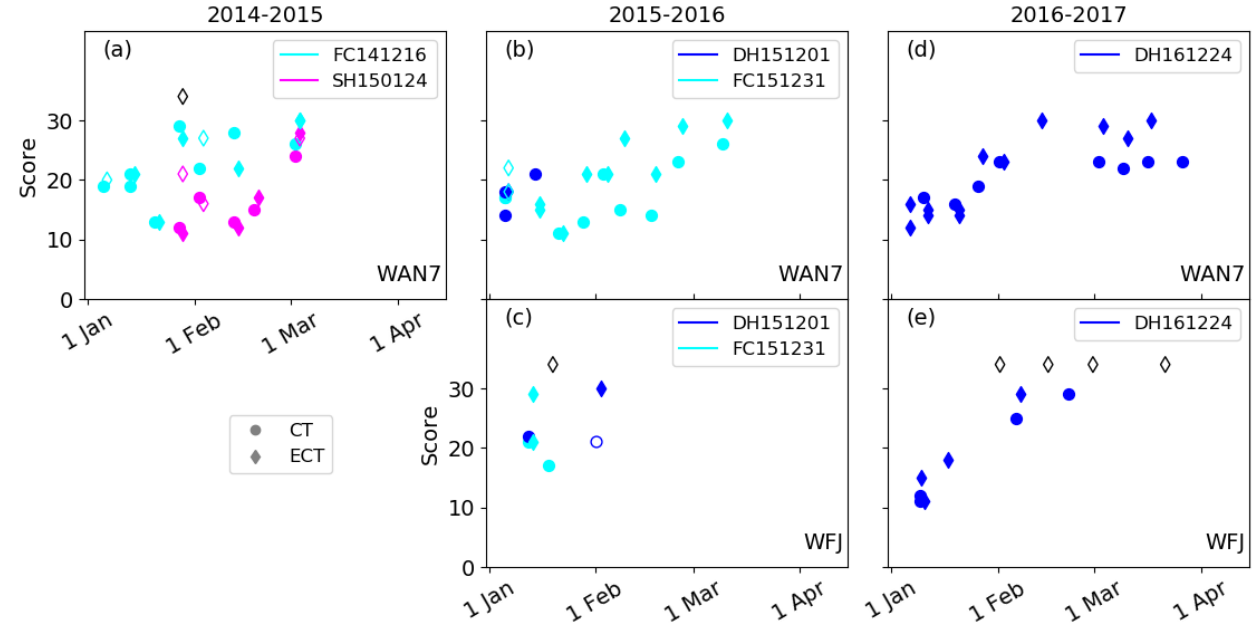

Figure 3. CT and ECT score (number of taps) for the winter seasons 2014-2015 (a: WAN7), 2015-2016 (b: WAN7; c: WFJ) and 2016-2017 (d: WAN7; e: WFJ). Shown are only the results of the persistent weak layers, which were also tracked in PST experiments. Filled markers correspond to the CT fracture type sudden collapse or sudden planar, or to full propagation in case of ECT. Black markers indicates no failure.

2d). During this winter, we only performed measurements at the WAN7 field site. A more detailed description of the weather development and weak layer formation can be found in Schweizer et al. (2016b).

Winter 2015-2016

In early November, a first snow storm deposited around 30 cm of snow at both field sites. A period of calm weather followed and large temperature gradients transformed the snow surface into a layer of depth hoar (DH151201). On 1 December 2015, local observers reported rain up to 2600 m a.s.l., forming a crust on top of DH151201. In mid-December, an additional 20 cm of snow accumulated on the crust, and subsequently transformed into a layer of faceted crystals during a clear weather period. This layer of facets was then covered by snow on 31 December 2015 (FC151231). From January 2016 on, no further prominent weak layer developed. These two persistent weak layers, below and above the crust, were observed at both field sites.

Winter 2016-17

This winter was relatively similar to the previous winter, starting with a shallow snowpack followed by a period of calm weather. Around 20-30 cm above the ground, a layer of DH crystals formed. This weak layer was covered by snow on 24 December

https://doi.org/10.5194/tc-2019-97
Preprint. Discussion started: 4 June 2019

The Cryosphere Discussions
Open Access
EGU

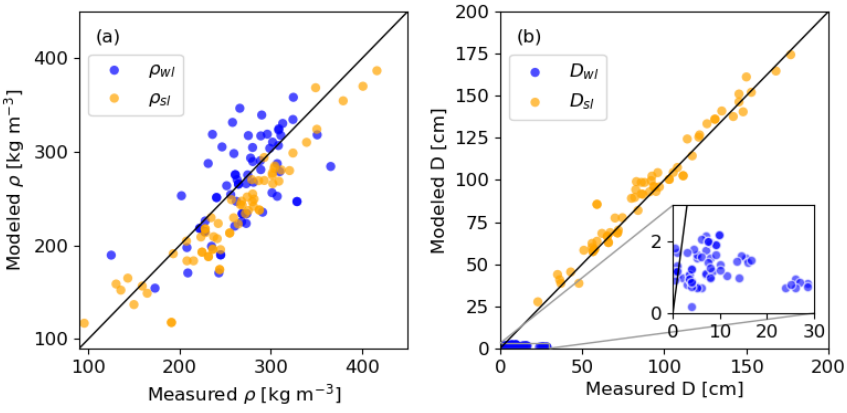

Figure 4. Comparison of (a) modeled to measured weak layer density ρ_{wl} and mean slab density ρ_{sl} and (b) weak layer thickness D_{wl} and slab thickness D_{sl}. Modeled properties were taken from SNOWPACK simulations while measured properties come from manually observed snow profiles. Black line is the 1:1 line.

2016 (DH161224). Between January and March 2017, several small snow storms occurred such that the snow height reached about 200 cm at the beginning of March. No further pronounced weak layers developed during this winter.

3.2 Modeled snow stratigraphy

For each site and winter season SNOWPACK reproduced the main stratigraphic features reasonably well (Figure 2 d-i). The overall hardness profiles agreed with the observations and the weak layers that were identified and tracked in the field were also present in the simulated profiles. In the winter 2015-2016, a rain crust at a depth of 25 cm was observed in the manually observed profiles at both sites. SNOWPACK did not simulate this rain crust but rather a thin layer of new snow, since the air temperature stayed well below zero degrees.

For the critical crack length parameterization, slab and weak layer properties are required. Most variables in Eq. (2) are related to density, which was also measured in the field. Modeled slab density ρ_{sl} agreed well (Figure 4a) with measured density ($r_p = 0.94$, $p << 0.05$ and $NRMSE = 0.13$), and the agreement for weak layer density ρ_{wl} was only slightly worse ($r_p = 0.61$, $p << 0.05$ and $NRMSE = 0.15$). Modeled slab thickness also agreed well (Figure 4b) with observed D_{sl} ($r_p = 0.98$, $p << 0.05$ and $NRMSE = 0.09$). Weak layer thickness, however, did not agree with observed thickness ($r_p = -0.14$, $p = 0.98$ and $NRMSE = 1.24$). While in the field weak layer thicknesses of up to 30 cm were recorded, D_{wl} ranged from 0.18 to 2.18 cm in the simulations.

3.3 Evolution of the critical crack length

PST experiments were conducted in the persistent weak layers described above. Observed critical crack lengths ranged from 17 to 121 cm and generally increased with time for all sites and seasons (Figure 5). Temporary decreases in r_c were sometimes

https://doi.org/10.5194/tc-2019-97
Preprint. Discussion started: 4 June 2019

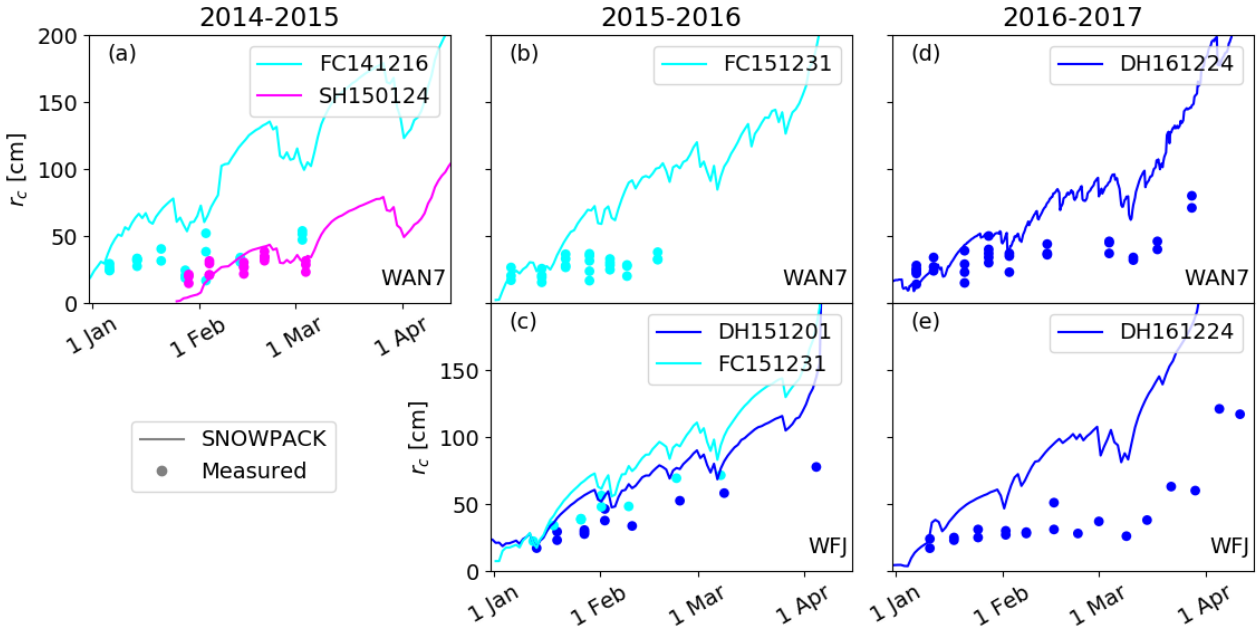

Figure 5. Evolution of the critical crack length r_c for the winter seasons 2014-2015 (a: WAN7), 2015-2016 (b: WAN7; c: WFJ) and 2016-2017 (d: WAN7; e: WFJ). Dots represent mean measured r_c values from PST experiments, lines represent modeled r_c values with layer properties from SNOWPACK using Eq. (2).

observed after pronounced precipitation events, as for example around 9 March 2017 (Figure 5 d,e). Depending on the weak layer and the field site, seasonal increases in observed r_c were more or less pronounced. For instance, r_c for layer FC151231 only slightly increased from 20 cm to 40 cm at WAN7 (Figure 5), whereas at WFJ the increase was more prominent (Figure 5 b,c). The largest increases in r_c were observed end of March and early April 2017.

The overall temporal trend of r_c (Eq. (2)) was reproduced when using layer properties from SNOWPACK ($r_p = 0.88$, $p << 0.05$; Figure 5). However, r_c was generally overestimated ($NRMSE = 1.80$; Figure 6) and simulated r_c values ranged from 4 to 468 cm. The only exception was for a layer of buried surface hoar (SH150124), for which observed and simulated r_c values corresponded well ($r_p = 0.91$, $p = 0.03$ and $NRMSE = 0.35$; Figure 5a). Modeled r_c values (Eq. (2)) were also calculated using layer properties from manually observed snow profiles, if data on thickness and density were available. Doing so, the discrepancies between modeled (Eq. (2)) and observed r_c values were even larger ($r_p = 0.75$, $p << 0.05$ and $NRMSE = 6.99$; Figure 6).

Clearly, the modeled critical crack length with layer properties either from SNOWPACK or from manual snow profiles overestimated observed critical crack lengths, especially later in the season. Since we used the same parameterizations for the required mechanical properties of snow, namely E and τ_p, we investigated differences in modeled and observed density or layer thickness more closely. While modeled slab and weak layer densities as well as slab thickness corresponded well

https://doi.org/10.5194/tc-2019-97
Preprint. Discussion started: 4 June 2019

The Cryosphere Discussions
Open Access
EGU

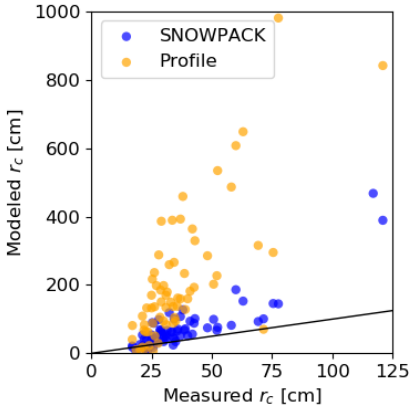

Figure 6. Modeled r_c values (Eq. (2)) with layer properties from SNOWPACK (blue dots) and from manual profiles (orange dots) with mean measured critical crack length from PST experiments. The black line is the 1:1 line.

with the observation (Figure 4), modeled and observed weak layer thickness were completely different (blue dots in Fig. 4b). Indeed, measured values of D_{wl} ranged from 0.5 to 30 cm, whereas in SNOWPACK D_{wl} ranged from 0.2 to 2.2 cm. These differences may be related to difficulties in assessing layer boundaries in manual snow profiles, but are primarily due to numerical boundary conditions limiting the thickness of layers in SNOWPACK. Furthermore, the weak layer shear modulus was taken as constant ($G_{wl} = 0.2$ MPa). This simplification does not account for the wide range of layer properties typically encountered in a natural snow cover. Thus, D_{wl} and G_{wl} in the parameterization of Gaume et al. (2017) are likely responsible for the observed discrepancies in modeled critical crack length.

3.4 Improvements to r_c parameterization

To improve the r_c parameterization we replaced the ratio $\frac{D_{wl}}{G_{wl}}$ with a parameter $F_{wl} = f(\rho_{wl}, gs_{wl})$, i.e. a function of density ρ_{wl} and the grain size gs_{wl} of the weak layer. $F_{wl} = \frac{D_{wl}}{G_{wl}}$ can be determined from mean $r_{c,obs}$ from PST measurements for each layer and each day in combination with layer properties σ_n, E' and τ_p from SNOWPACK using Eq. (2):

$$F_{wl} = r_{c,obs}^2 \cdot \frac{\sigma_n}{2\tau_p} \cdot \frac{1}{E' D_{sl}} \tag{6}$$

Based on the 68 mean observed critical crack lengths in the winter 2014-2015 to 2016-2017 and slab and weak layer variables from SNOWPACK simulations, F_{wl} ranged between 4.02×10^{-9} and 3.41×10^{-7} m Pa^{-1} (blue dots in Fig. 7). We then fitted the values of F_{wl} to a power law function

$$F_{wl} = a \left(\left(\frac{\rho_{wl}}{\rho_{ice}} \right)^x \left(\frac{gs_{wl}}{gs_0} \right)^y \right)^b \tag{7}$$

with the fit parameters a and b. To normalize grain size we select $gs_0 = 0.00125$ m according to Schweizer et al. (2008). With x and y integers ranging from -3 to 3, we evaluated 48 fit functions. Therefore, we calculated POD (Eq. (4)) and FAR (Eq.

https://doi.org/10.5194/tc-2019-97
Preprint. Discussion started: 4 June 2019

The Cryosphere
Discussions
Open Access
EGU

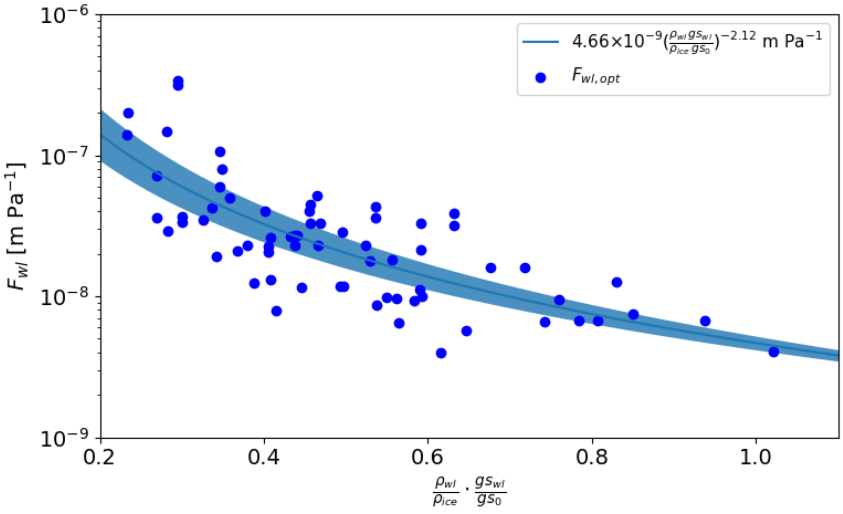

Figure 7. Parameter F_{wl}^{opt} (Eq. (6)) with modeled normalized weak layer density $\frac{\rho_{wl}}{\rho_{ice}}$ times normalized grain size $\frac{gs_{wl}}{gs_0}$. The blue line shows a power law fit for F_{wl} (Eq. (7)). Blue area is the 95% confidence interval of the 10-fold cross-validation.

(5)) values for all field days ($m = 47$) from the automatic weak layer detection method (see Sect. 2.5). The best performance, i.e. high POD and low FAR, was obtained with $x = y = 1$, namely a POD of 0.91 and a FAR of 0.47 (Figure 8). The original parameterization of Gaume et al. (2017) performed poorly in terms of weak layer detection with a relatively low POD of 0.26 and a high FAR of 0.89. To exemplify these differences, on 13 February 2015, using the original parameterization (Eq. (2)), only one (d=1) of the two tested weak layers (nd=1) was within the five weakest layers (Figure 9a), resulting in a POD of 0.5 and a FAR of 0.8 for that single day. In contrast, using the fit function with $x = y = 1$, both weak layers were detected within the first three weakest layers, resulting in a POD of 1 and a FAR of 0.33. We therefore suggest a new parameterization of r_c, where $\frac{D_{wl}}{G_{wl}}$ in Eq. (2) is replaced by F_{wl}:

$$r_c = \sqrt{E' D_{sl} F_{wl}} \sqrt{\frac{2\tau_p}{\sigma_n}}, \tag{8}$$

where F_{wl} is given by:

$$F_{wl} = a \left(\frac{\rho_{wl}}{\rho_{ice}} \cdot \frac{gs_{wl}}{gs_0} \right)^b \text{[m Pa}^{-1}\text{]}, \tag{9}$$

where $a = 4.7 \times 10^{-9} \pm 0.3 \times 10^{-9}$ m Pa^{-1} and $b = -2.1 \pm 0.1$ are the mean fit parameters obtained with 10-fold cross-validation (Wilks, 2011). For this, we randomly split the joint data set into 10 groups, fitted F_{wl} with nine groups and tested the fit function on the excluded group. After performing this ten times with each group serving as test group, we averaged the fit parameters and performance values. This yielded an average $NRMSE = 0.28 \pm 0.07$ for modeled r_c from SNOWPACK simulation using Eq. (8). Compared to the original parameterization (Eq. (2)) with an $NRMSE = 1.80$, the results highly

https://doi.org/10.5194/tc-2019-97
Preprint. Discussion started: 4 June 2019

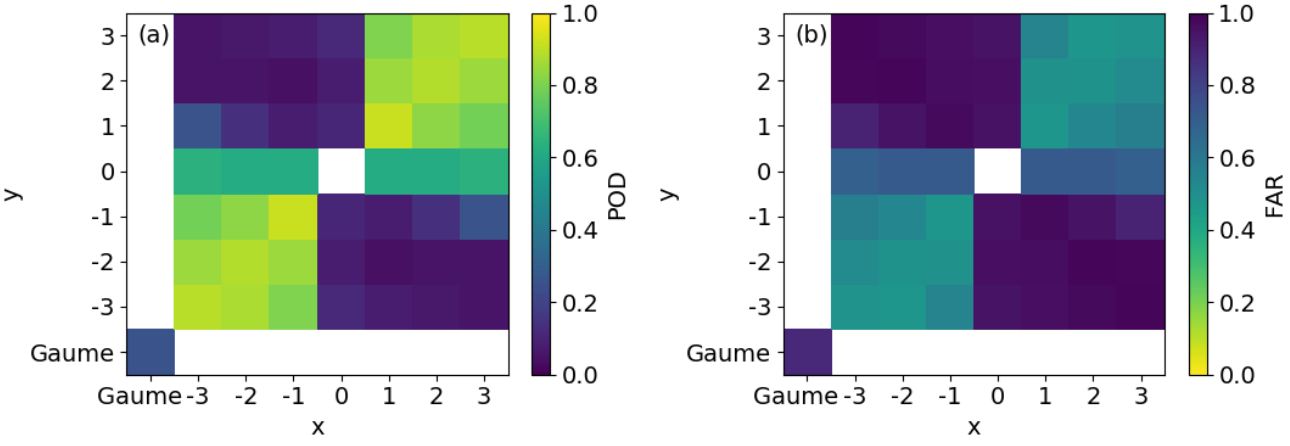

Figure 8. (a) POD and (b) FAR values for the 47 field days with exponents x and y for the power law fit function $F_{wl} = a\,(\rho_{wl}^{x} gs_{wl}^{y})^{b}$. Values for x and y ranged from -3 to 3. The original parametrization of Gaume et al. (2017) (Eq. (2)) is shown in the lower left corner.

improved. For SNOWPACK, values of r_c ranged from 10 to 123 cm ($r_p = 0.90$, $p << 0.05$) using Eq. (8) (blue dots in Fig. 10). The discrepancies between modeled values of critical crack length from manually observed snow profiles and measured r_c values (orange dots in Fig. 10) were also removed using Eq. (8), with modeled r_c values ranging from 4 to 120 cm ($r_p = 0.67$, $p << 0.05$ and $NRMSE = 0.52$). Also, the match between observed and modeled time series of r_c using SNOWPACK layer properties for the individual weak layers was substantially better when using Eq. (8) (Figure 11).

4 Discussion

Based on our current understanding of avalanche release processes, failure initiation in the weak layer below the slab is followed by rapid crack propagation across the slope before snow masses start moving downhill (e.g. Schweizer et al., 2003a; van Herwijnen and Jamieson, 2007). Several failure initiation criteria, e.g. SN38 or SK38, have been implemented in SNOWPACK (Lehning et al., 2004; Monti et al., 2016). To validate these stability indices, previous studies relied on a variety of field measurements, including shear frame measurements, stability tests, manual snow profiles and avalanche observations, to compare modeled stability metrics with observations. Whereas the SK38 as introduced by Föhn (1987) and refined by Jamieson and Johnston (1998) is closely related to avalanche activity, SN38 is a rather poor predictor of natural avalanche release (Gauthier et al., 2010). While the modeled SK38 performed poorly in terms of identifying potential weak layers, combining it with structural parameters, e.g. differences in grain sizes or hand hardness, the performance improved (Schweizer et al., 2006; Schweizer and Jamieson, 2007). However, failure initiation is only one piece of the puzzle and crack propagation is another important process to consider in snow instability evaluation. Observed higher and lower propagation propensity was predicted by PST experiments and therefore the critical crack length provides valuable information on crack propagation (Gauthier and

https://doi.org/10.5194/tc-2019-97
Preprint. Discussion started: 4 June 2019

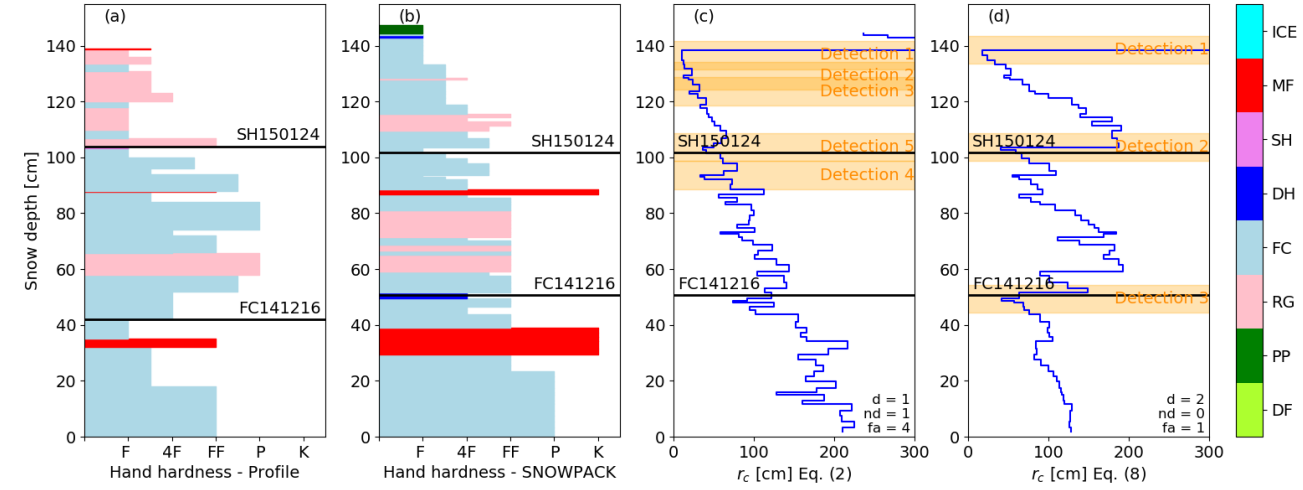

Figure 9. Observed (a) and simulated (b) hand hardness profiles on 13 February 2015 at WAN7. Colors indicate grain type. Corresponding vertical r_c profiles using layer properties from SNOWPACK for (c) the parameterization of Gaume et al. (2017) (Eq. (2)), and (d) the optimized parameterization (Eq. (8)). Black lines show the weak layers on which PST experiments were performed. Orange bars show the automatically detected weak layers (local minima) in the r_c profiles.

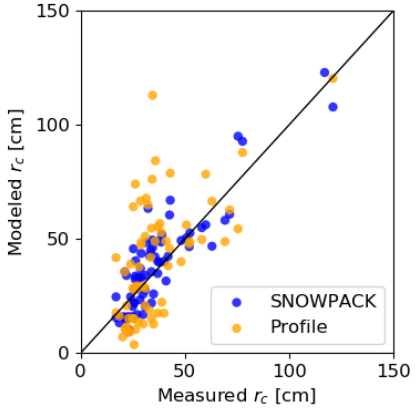

Figure 10. Modeled values of critical crack length (Eq. (8)) with layer properties from SNOWPACK (blue dots) and from manually observed profiles (orange dots) vs. mean critical crack length from PST experiments. The black line is the 1:1 line.

Jamieson, 2008b). PST experiments furthermore allow to directly compare measurements to the critical crack length modeled by SNOWPACK. This greatly facilitates the validation, especially when performing the measurements directly next to an automatic weather station used to drive SNOWPACK, as was done in this study.

PST experiments only provide a measure for the critical crack length in layers that are prone to crack propagation. Such layers are typically soft (hand hardness index ≤ 2) and consist of rather large crystals, as typically found in the failure layers

https://doi.org/10.5194/tc-2019-97
Preprint. Discussion started: 4 June 2019

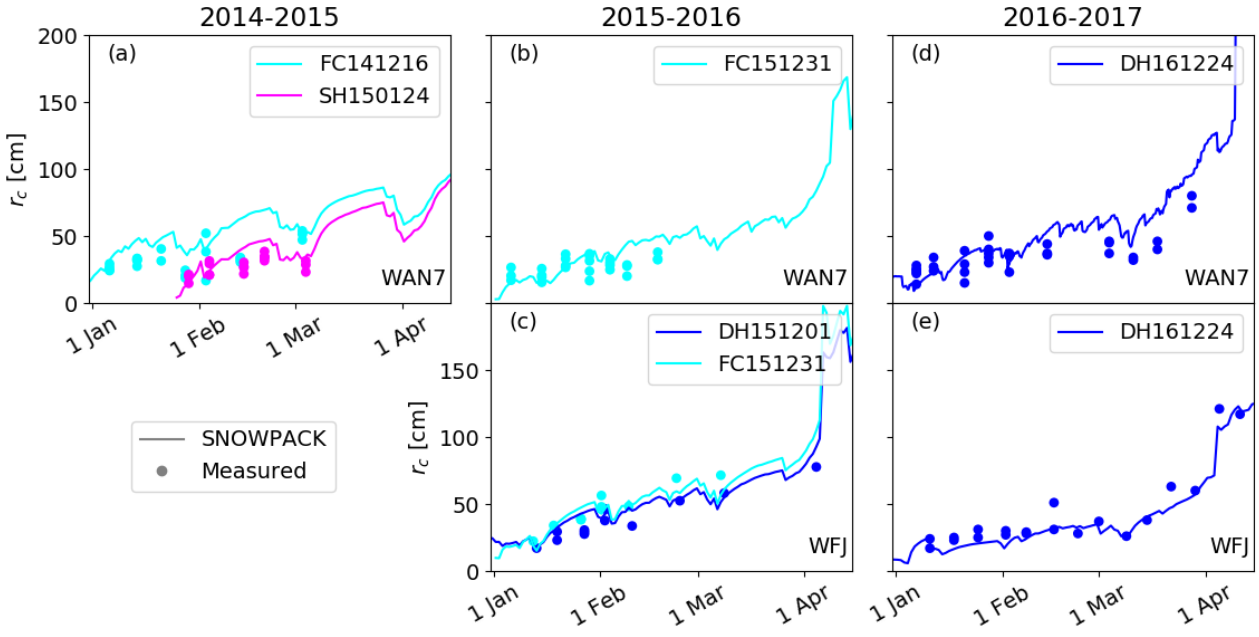

Figure 11. Evolution of the critical crack length at WAN7 (top) and WFJ (bottom) for the winter seasons 2014-2015 (a: WAN7), 2015-2016 (b: WAN7; c: WFJ) and 2016-2017 (d: WAN7; e: WFJ). Dots represent mean measured r_c values from PST experiments, lines represent modeled r_c values with layer properties from SNOWPACK using Eq. (8).

of avalanches (Schweizer and Jamieson, 2003; van Herwijnen and Jamieson, 2007). Performing a PST in other layers, such as for instance a layer of small rounded grains, generally does not yield any result for the critical crack length. The only microstructural dependence in the original parameterization of Gaume et al. (2017) (Eq. (2)) was through the grain type dependence of the shear strength τ_p developed by Jamieson and Johnston (2001) and implemented in SNOWPACK. As differences in τ_p based on grain type are rather modest for densities below 300 kg m^{-3} (Figure 1), the modeled critical crack length mainly increased with depth (Figure 9c) which led to a low POD=0.26 and high FAR=0.89 based on the 47 field days. Furthermore, modeled r_c became unrealistically large late in the season (Figure 5). Our proposed refined parameterization (Eq. (8)) greatly improved the results as it removed two variables of the original parameterization (Eq. (2)), which were not sufficiently well represented in SNOWPACK.

The first variable was weak layer thickness D_{wl}. The large discrepancies between observed and modeled D_{wl} showed that simply using modeled D_{wl} results in poor estimates of r_c (Figure 4). While a layer per definition should differ from adjacent layers in density or microstructure (Fierz et al., 2009), layer thicknesses are constrained by numerical stability in SNOWPACK and the subjectiveness of the observer in manually observed snow profiles. To develop the original r_c parameterization (Eq. (2)), Gaume et al. (2017) performed numerical simulations using an idealized structure of the weak layer and D_{wl} was closely linked to collapse height. Indeed, when r_c is reached in a PST experiment, crack propagation occurs inducing the structural

https://doi.org/10.5194/tc-2019-97
Preprint. Discussion started: 4 June 2019

collapse of the weak layer (e.g. van Herwijnen and Jamieson, 2005; van Herwijnen et al., 2010). The collapse height is believed to contribute to extensive fracture propagation (Jamieson and Schweizer, 2000; van Herwijnen and Jamieson, 2005; van Herwijnen et al., 2010). However, collapse heights are generally around 1 to 10 mm in real PST experiments (van Herwijnen and Jamieson, 2005), i.e. on the order of the grain size rather than D_{wl}. While thus far it remains unclear whether the collapse height relates to r_c and how it scales with grain size, it is plausible to consider grain size rather than weak layer thickness in the parameterization. Moreover, structural length, crystal size and grain size have been previously introduced to improve the paramterizations of mechanical properties (e.g. Proksch et al., 2015; Schulson, 2001; Schweizer et al., 2004).

The second variable in Eq. (2) was the shear modulus of the weak layer G_{wl}. Thus far, there are very few measurements of G_{wl} (Föhn et al., 1998; Reiweger et al., 2010) and therefore G_{wl} was kept constant in the original parameterization. Nevertheless, one would expect G_{wl} to increase with increasing density, similar to E' (Scapozza, 2004; van Herwijnen et al., 2016). This would in part compensate the exaggerated seasonal increase in modeled r_c (Figure 12). In the absence of a sound G_{wl} parameterization, replacing G_{wl} with a term depending on ρ_{wl} to model r_c therefore seems plausible.

Thus, by replacing the poorly constrained $\frac{D_{wl}}{G_{wl}}$ term with Eq. (9), the temporal increase of r_c was less pronounced with increasing density, resulting in more realistic seasonal trends (Figure 11). Furthermore, r_c values decreased with increasing grain size, which greatly improved the performance of weak layer detection (Figure 8).

The critical crack length can be calculated for every simulated snow layer (Figure 9d). However, this does not mean that in each layer a crack will actually propagate. Currently, it is not possible to distinguish simulated snow layers with high propagation propensity from others. We therefore chose a simple local minimum approach to automatically detect weak layers. The optimized parameterization (Eq. (8)) increased the POD from 0.26 to 0.91 compared to Eq. (2). Hence, modeled critical crack length can properly represent observed results from snow instability tests and identify weaknesses within the simulated profile.

The seasonal evolution of r_c simulated with SNOWPACK using Eq. (8) for WFJ 2015-2016 showed a general increase of r_c for each layer (Figure 12). With increasing snow depth due to precipitation, r_c for each layer temporally decreased (e.g. at the beginning of February and March). The weak base in the lower 40 cm of the snowpack, which was tracked with the PST experiments, consistently showed lower r_c values than the overlying slab in the simulation. The simulation also showed weaknesses, which formed later in the season e.g. a layer that had formed on 31 January at the snow surface at around 120 cm. Although these layers might have been weak layers, they were not contained in our data set of PST experiments and therefore counted as false alarms.

5 Conclusions

During three winter seasons we monitored the evolution of the critical crack length r_c with PST experiments in persistent weak layers at two field sites above Davos, Switzerland. On 47 days, we collected data on 7 distinct persistent weak layers. Using data from 145 PST experiments, we showed that a recently suggested model to calculate r_c from layer properties (Gaume et al.,

https://doi.org/10.5194/tc-2019-97
Preprint. Discussion started: 4 June 2019

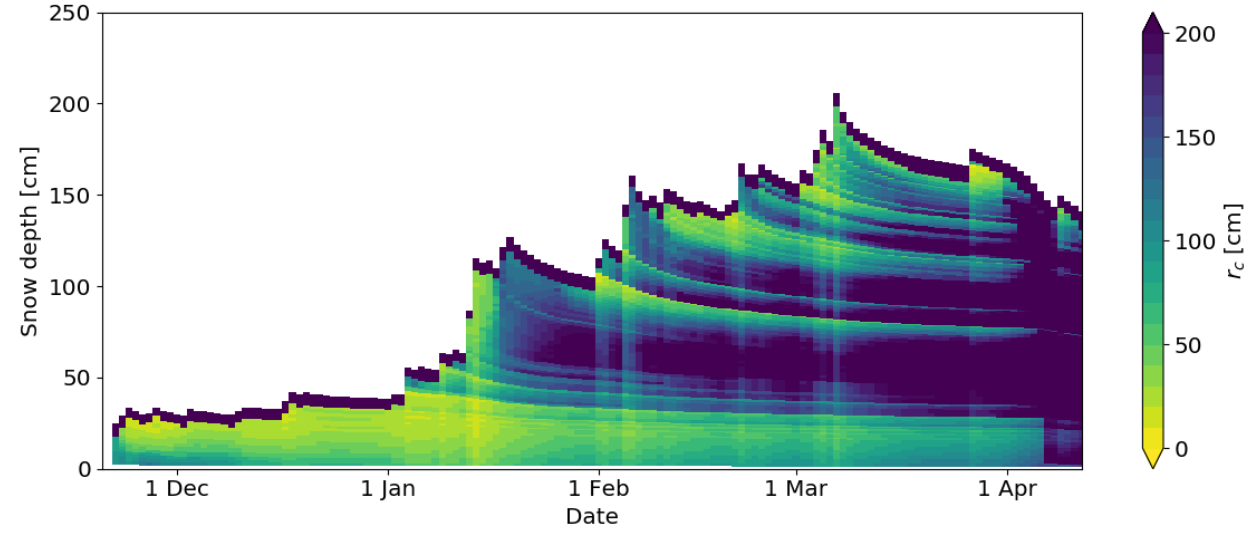

Figure 12. Temporal evolution of the vertical profile of the critical crack length modeled with SNOWPACK using Eq. (8) for WFJ 2015-2016.

2017) generally overestimated the observed critical crack length, especially later in the season. The discrepancies are likely related to the weak layer thickness D_{wl} and the shear modulus of the weak layer G_{wl}.

We therefore suggested an improved parameterization including weak layer grain size and weak layer density instead of D_{wl} and G_{wl} (Eq. (8)). The grain size term in the improved r_c parameterization (Eq. (8)) allowed us to implicitly account for snow microstructure. This resulted in lower r_c values for layers with larger grains, in line with our field experience. This also improved the automated weak layer detection within simulated snow profiles using a simple local minimum approach. The critical crack length can either be modeled with simulated layer properties from the snow cover model SNOWPACK, or from data from manual snow pit observations. In both cases, Eq. (8) greatly improved the match between observed and modeled r_c values and improved the representation of the observed seasonal evolution of the critical crack length. However, we want to highlight that the parameterization was developed based on data of weak layers of large faceted grains and could further be improved by sampling a greater diversity of weak layers.

The critical crack length relates to the onset of crack propagation and is therefore an important parameter to assess snow instability. However, a snowpack is only prone to avalanche release if conditions for failure initiation and crack propagation are fulfilled. For the instability criteria in SNOWPACK, these conditions still need to be defined and verified with independent data. Clearly, the complex problem of automatically identifying weak layers and evaluating their stability in simulated snow profiles is not yet solved. Nevertheless, our results are an encouraging step in the right direction.

Code availability. Data of PST experiments and snow pit data for winter season 2014-2015 at the field site WAN7 can be found online at https://doi.org/doi:10.5194/tc-10-2637-2016-supplement. Data on the remaining PST experiments, snow pits and weather data of AWS

https://doi.org/10.5194/tc-2019-97
Preprint. Discussion started: 4 June 2019

WAN7 are available upon request from B. Richter. Weather data of AWS WFJ can be found online at https://doi.org/doi:10.16904/1. The numerical snow cover model SNOWPACK can be downloaded from http://models.slf.ch/p/snowpack/.

Competing interests. The authors declare that they have no conflict of interests.

Acknowledgements. We would like to thank all colleagues involved in the field campaigns, in particular Stephanie Mayer and Konstantin Nebel. Bettina Richter has been supported by a grant of the Swiss National Science Foundation (200021_169641).

https://doi.org/10.5194/tc-2019-97
Preprint. Discussion started: 4 June 2019

References

Bartelt, P. and Lehning, M.: A physical SNOWPACK model for the Swiss avalanche warning Part I: Numerical model, Cold Reg. Sci. Technol., 35, 123–145, 2002.

Brun, E., David, P., and Sudul, M.: A numerical-model to simulate snow-cover stratigraphy for operational avalanche forecasting, J. Glaciol., 38, 13–22, 1992.

Chalmers, T. S.: Forecasting shear strength and skier-triggered avalanches for buried surface hoar layers, MSc thesis, Dept. of Civil Eng. University of Calgary, Calgary, Canada, 2001.

Durand, Y., Giraud, G., Brun, E., Merindol, L., and Martin, E.: A computer-based system simulating snowpack structures as a tool for regional avalanche forecasting, J. Glaciol., 45, 469–484, 1999.

Fierz, C., Armstrong, R., Durand, Y., Etchevers, P., Greene, E., McClung, D., Nishimura, K., Satyawali, P., and Sokratov, S.: The international classification for seasonal snow on the ground, HP-VII Technical Document in Hydrology, 83. UNESCO-IHP, Paris, France, p. 90, 2009.

Föhn, P.: The "Rutschblock" as a pratical tool for slope stability evaluation, IAHS-AISH Publ., 162, 223–228, 1987.

Föhn, P., Camponovo, C., and Krüsi, G.: Mechanical and structural properties of weak snow layers measured in situ, Ann. Glaciol., 26, 1–6, 1998.

Gaume, J., van Herwijnen, A., Chambon, G., Wever, N., and Schweizer, J.: Snow fracture in relation to slab avalanche release: critical state for the onset of crack propagation, The Cryosphere, 11, 217–228, 2017.

Gauthier, D. and Jamieson, B.: Evaluating a prototype field test for weak layer fracture and failure propagation, Proceedings of International Snow Science Workshop, Telluride, CO, USA, pp. 107–116, 2006.

Gauthier, D. and Jamieson, B.: Evaluation of a prototype field test for fracture and failure propagation propensity in weak snowpack layers, Cold Reg. Sci. Technol., 51, 87–97, 2008a.

Gauthier, D. and Jamieson, B.: Frature propagation propensity in relation to snow slab avalanche release: Validating the propagation saw test, Geophysical Research Letters, 35, L13 501, 2008b.

Gauthier, D., Brown, C., and Jamieson, B.: Modeling strength and stability in storm snow for slab avalanche forecasting, Cold Reg. Sci. Technol., 62, 107 – 118, 2010.

Giraud, G. and Navarre, J.: MEPRA et le risque de déclenchement accidentel d'avalanches, in: Les apports de la recherche scientifique à la sécurité neige, glace et avalanche. Actes de Colloque, Chamonix 30 mai-3 juin, 1995, pp. 145–150, 1995.

Jamieson, J. and Johnston, C.: Refinements to the stability index for skier-triggered dry-slab avalanches, Ann. Glaciol., 26, 296–302, 1998.

Jamieson, J. and Johnston, C.: Evaluation of the shear frame test for weak snowpack layers, Ann. Glaciol., 32, 59–69, 2001.

Jamieson, J. B. and Schweizer, J.: Texture and strength changes of buried surface-hoar layers with implications for dry snow-slab avalanche release, J. Glaciol., 46, 151–160, 2000.

Lafaysse, M., Morin, S., Coléou, C., Vernay, M., Serça, D., Besson, F., Willemet, J.-M., Giraud, G., Durand, Y., and Météo-France, D.: Towards a new chain of models for avalanche hazard forecasting in French mountain ranges, including low altitude mountains, in: Proceedings of International Snow Science Workshop Grenoble–Chamonix Mont-Blanc, pp. 162–166, 2013.

Lehning, M., Bartelt, P., Brown, B., and Fierz, C.: A physical SNOWPACK model for the Swiss avalanche warning: Part III: meteorological forcing, thin layer formation and evaluation, Cold Reg. Sci. Technol., 35, 169 – 184, 2002.

https://doi.org/10.5194/tc-2019-97
Preprint. Discussion started: 4 June 2019

Lehning, M., Fierz, C., Brown, B., and Jamieson, B.: Modeling snow instability with the snow-cover model SNOWPACK, Ann. Glaciol., 38, 331–338, 2004.

McClung, D. M. and Schweizer, J.: Skier triggering, snow temperatures and the stability index for dry-slab avalanche initiation, J. Glaciol., 45, 190–200, 1999.

Monti, F., Gaume, J., van Herwijnen, A., and Schweizer, J.: Snow instability evaluation: calculating the skier-induced stress in a multi-layered snowpack, Natural Hazards and Earth System Sciences, 16, 775–788, 2016.

Proksch, M., Löwe, H., and Schneebeli, M.: Density, specific surface area and correlation length of snow measured by high-resolution penetrometry, Journal of Geophysical Research, 120, 346–362, https://doi.org/10.1002/2014JF003266, 2015.

Reiweger, I., Schweizer, J., Ernst, R., and Dual, J.: Load-controlled test apparatus for snow, Cold Reg. Sci. Technol., 62, 119–125, 2010.

Reuter, B. and Schweizer, J.: Describing snow instability by failure initiation, crack propagation, and slab tensile support, Geophysical Research Letters, 45, 7019–7027, 2018.

Reuter, B., Schweizer, J., and van Herwijnen, A.: A process-based approach to estimate point snow instability, The Cryosphere, 9, 837–847, 2015.

Scapozza, C.: Entwicklung eines dichte- und temperaturabhängigen Stoffgesetzes zur Beschreibung des visko-elastischen Verhaltens von Schnee, Ph.D. thesis, ETH Zürich, 2004.

Schulson, E. M.: Brittle failure of ice, Engineering Fracture Mechanics, 68, 1839 – 1887, 2001.

Schweizer, J. and Jamieson, B.: Snowpack properties for snow profile analysis, Cold Reg. Sci. Technol., 37, 233–241, 2003.

Schweizer, J. and Jamieson, B.: Snowpack tests for assessing snow-slope stability, Ann. Glaciol., 51, 187–193, 2010.

Schweizer, J. and Jamieson, J.: A threshold sum approach to stability evaluation of manual snow profiles, Cold Reg. Sci. Technol., 47, 50–59, 2007.

Schweizer, J., Jamieson, J., and Schneebeli, M.: Snow avalanche formation, Rev. Geophys., 41, 1016, 2003a.

Schweizer, J., Kronholm, K., and Wiesinger, T.: Verification of regional snowpack stability and avalanche danger, Cold Reg. Sci. Technol., 37, 277–288, 2003b.

Schweizer, J., Michot, G., and Kirchner, H. O.: On the fracture toughness of snow, Ann. Glaciol., 38, 1–8, 2004.

Schweizer, J., Bellaire, S., Fierz, C., Lehning, M., and Pielmeier, C.: Evaluating and improving the stability predictions of the snow cover model SNOWPACK, Cold Reg. Sci. Technol., 46, 52–59, 2006.

Schweizer, J., Reuter, B., van Herwijnen, A., and Gaume, J.: Avalanche release 101, in: Proceedings of the International Snow Science Workshop, Breckenridge CO, U.S.A., pp. 1–11, 2016a.

Schweizer, J., Reuter, B., van Herwijnen, A., Richter, B., and Gaume, J.: Temporal evolution of crack propagation propensity in snow in relation to slab and weak layer properties, The Cryosphere, 10, 2637–2653, 2016b.

Schweizer, J., McCammon, I., and Jamieson, J. B.: Snowpack observations and fracture concepts for skier-triggering of dry-snow slab avalanches, Cold Reg. Sci. Technol., 51, 112–121, 2008.

Sigrist, C. and Schweizer, J.: Critical energy release rates of weak snowpack layers determined in field experiments, Geophysical Research Letters, 34, L03 502, 2007.

https://doi.org/10.5194/tc-2019-97
Preprint. Discussion started: 4 June 2019

Simenhois, R. and Birkeland, K. W.: The Extended Column Test: Test effectiveness, spatial variability, and comparison with the Propagation Saw Test, Cold Reg. Sci. Technol., 59, 210–216, 2009.

Techel, F., Jarry, F., Kronthaler, G., Mitterer, S., Nairz, P., Pavšek, M., Valt, M., and Darms, G.: Avalanche fatalities in the European Alps: long-term trends and statistics, Geographica Helvetica, 71, 147–159, 2016.

van Herwijnen, A. and Jamieson, B.: High-speed photography of fractures in weak snowpack layers, Cold Reg. Sci. Technol., 43, 71–82, 2005.

van Herwijnen, A. and Jamieson, B.: Snowpack properties associated with fracture initiation and propagation resulting in skier-triggered dry snow slab avalanches, Cold Reg. Sci. Technol., 50, 13–22, 2007.

van Herwijnen, A. and Jamieson, B.: Fracture character in compression tests, Cold Reg. Sci. Technol., 47, 60–68, 2007.

van Herwijnen, A., Gaume, J., Bair, E. H., Reuter, B., Birkeland, K. W., and Schweizer, J.: Estimating the effective elastic modulus and specific fracture energy of snowpack layers from field experiments, J. Glaciol., 62, 997–1007, 2016.

van Herwijnen, A., Schweizer, J., and Heierli, J.: Measurement of the deformation field associated with fracture propagation in weak snowpack layers, J. Geophys. Res. - Earth, 115, F03 042, 2010.

Vernay, M., Lafaysse, M., Mérindol, L., Giraud, G., and Morin, S.: Ensemble forecasting of snowpack conditions and avalanche hazard, Cold Reg. Sci. Technol., 120, 251 – 262, 2015.

Vionnet, V., Brun, E., Morin, S., Boone, A., Martin, E., Faroux, S., Moigne, P. L., and Willemet, J.-M.: The detailed snowpack scheme Crocus and its implementation in SURFEX v7.2, Geosci. Model. Dev., 5, 773–791, 2012.

Wever, N., Schmid, L., Heilig, A., Eisen, O., Fierz, C., and Lehning, M.: Verification of the multi-layer SNOWPACK model with different water transport schemes, The Cryosphere, 9, 2271–2293, 2015.

Wilks, D. S.: Statistical methods in the atmospheric sciences, vol. 100, Academic press, 2011.

WSL Institute for Snow and Avalanche Research SLF: WFJ_MOD: Meteorological and snowpack measurements from Weissfluhjoch, WSL Institute for Snow and Avalanche Research SLF, https://doi.org/10.16904/1, 2015.